



## ESTIMATION OF THE OPTIMUM BED THICKNESS OF A FLOW-THROUGH POROUS ELECTRODE (FTPE) WORKING UNDER MASS TRANSFER CONTROL

Qasim J. M. Slaiman<sup>\*</sup>, Sarmad Talib Najim<sup>\*</sup>, Aws Abdulmahdi Sadeq<sup>\*\*</sup>

<sup>\*</sup> Collage of Engineering/Chemical Eng. Dep. /Nahrain University

<sup>\*\*</sup> Ministry of Oil/ Iraqi Drilling Company

### ABSTRACT:

In this paper, a theoretical analysis of optimum bed thickness operates under mass transfer control for realizing a high efficiency and reaction conversion of an electrochemical reactor has been made based on flow-through porous electrode (FTPE) configuration. Many models have been used to represent the optimum bed thickness by taking a look into previous works concerned and collecting all related information, data, and models. The parameters that affect the optimum bed thickness have been visualized and reviewed, and almost all of them have been examined by experimental data from different sources and based on the various models. It has been found that the increase in electrolyte flow rate, concentration, limiting current density, and specific surface area reduce the optimum bed thickness, and the increase in electrolyte conductivity, void fraction, and overpotential range increases optimum bed thickness. The most important design parameter that has a great effect on optimum bed thickness is found to be the electrolyte flow rate for any certain operation. It has been concluded that the most appropriate two models to represent the optimum bed thickness of FTPE electrochemical reactor operating under mass transfer control based on the results are those predicted theoretically and stated by Kreysa in (1978) and Doherty et al. in (1996).

:

.(FTPE)

specific surface area limiting current density

)

(

(Flow-through)

Doherty et al. (1978) Kreysa

.(1996)

**Keywords:** Optimum bed thickness; Packed bed; Porous electrode; Flow-through; Mass transfer

## 1- INTRODUCTION

Packed bed electrodes can be used for electrochemical recovery of heavy metals from a variety of industrial and laboratory model solutions (Bennion and Newman, 1972; Doherty et al., 1996; El-Deab et al., 1999; Gaunand et al., 1977; Lanza and Bertazzoli, 2000; Matloz and Newman, 1986; Podlaha and Fenton, 1995; Ponce de León and Pletcher, 1996; Saleh, 2004; Soltan et al., 2003; Trainham and Newman, 1977). The packed bed electrode forms a porous flow-through configuration providing large surface area usually depleting the concentration of metal ions below 0.1 ppm.

Some studies have reported that flow-through configurations suffer from non-uniform potential and current distribution (Bennion and Newman, 1972; Doherty et al., 1996; El-Deab et al., 1999; Gaunand et al., 1977; Matloz and Newman, 1986; Saleh, 2004; Sioda, 1971; Trainham and Newman, 1977). Newman et al. in 1962 demonstrated this problem when Tafel kinetic was coupled with significant solid phase (electrode material) and electrolyte resistivity. In another paper related to the potential and current distribution, Bennion and Newman (1972) used the deposition of copper ions on carbon flakes to study the design principles of flow-through porous electrodes.

The authors concluded that electrolyte flow rate and bed thickness determine the ohmic potential drop within the porous electrode. Another conclusion was that the potential difference between the carbon matrix and the solution at all points within the porous electrode should be sufficient, but not too large to ensure deposition without hydrogen evolution. Sabacky and Evans (1979) used a fluidised copper particles cathode for copper recovery and reported that the efficiency and power consumption depended on copper and acid concentration, particle size, resistivity of the electrolyte and superficial current density. Kreysa in (1978) studied the kinetic behavior of packed and fluidized bed electrodes. A macro-kinetic model of three-dimensional electrodes was established by introducing overpotential distribution within the electrode into the micro-kinetic rate equation. The developed model was used to derive analytical expression from limiting diffusion current for calculating the optimum bed depth for both packed and fluidized bed electrodes in terms of geometric, hydrodynamics, and kinetic parameters. Kreysa and Jüttner in (1993) in a study for flow-by three-dimensional electrode of cylindrical geometry operating under limiting current conditions re-introduced the arrangement of electrodes

with respect to the direction of the current flow, electrolyte flow, and electrode position. Comparisons have been made among various types of electrode arrangements. Optimum bed thickness also had been investigated for both cylindrical and rectangular arrangements for various electrolyte conductivities. The model used for calculation was similar to that predicted by Kreysa (1978) with a little difference due to ignoring effects of void fraction.

Doherty et al. in (1996) presented a numerical model of flow-through porous electrodes simulates the distribution of potential and current density within a porous electrode. The model includes consideration of the electron transfer control regime of the electrode reaction, mass transport limitations and the finite conductivity of the electrode material. They re-introduced the expression predicted by Kreysa (1978) for calculation of the optimum bed depth in terms of specific surface area instead of particle size diameter. They concluded that at high electrode conductivities the optimum length is much less sensitive to electrode depth, whereas, at low conductivities the contrary is true. Therefore, greater accuracy is required when designing porous electrodes with very high porosities and, thus, low electrode conductivities, in order to achieve the optimum electrode depth.

Masiley and Pouddubny in (1997) presented mathematical simulation of the FTPE operation on the basis of one dimensional model with uniform conducting matrix and the cathode process involving the main and side reaction. They introduced the optimum bed thickness as a part of its total thickness  $L$  proportional to the integral mean value of the ratio of local current of the target reaction to its limiting diffusion value. They also studied the effect of solid and liquid phase conductivity on the effective electrode layer operating under limiting diffusion current. The expression that they obtained in case of solid phase conductivity is much higher than that for electrolyte and was quite similar to that used by Kreysa and Jüttner (1993).

In a more recent paper, Saleh in (2004) re-introduced the concept of effectiveness factor as the ratio between the total obtainable limiting current and the maximum limiting current in absence of ohmic drop. The study was based on the deposition of zinc in alkaline solution where the hydrogen evolution reaction and the deposition of zinc take place at similar potential. Saleh concluded that hydrogen evolution accentuates the ohmic effect. Similarly, Like and Langer in

(1991) discussed the internal ohmic limits in a flow-through porous electrode using Tafel kinetics. They showed that during the electrolysis, thinner electrodes help to maximize the current density.

Nava et al. in (2008) discussed the use of potential distribution analysis during the deposition of metal ions, at limiting current conditions and determine the optimum electrode thickness at which no hydrogen evolution occurs. The potential distribution studies were carried out on stainless-steel fibres of three different surface areas. The fibres were used as cathodic porous electrodes during the deposition of Ag(I) ions contained in 0.1 mol dm<sup>-3</sup> KNO<sub>3</sub> and 0.6 mol dm<sup>-3</sup> NH<sub>4</sub>OH electrolyte. The comparison of both, experimental and theoretical potential distributions showed that flow rate and specific surface area of the electrode determine the potential drop within the packed bed cathode and therefore the effective thickness of the porous bed electrode at which hydrogen evolution can be avoided.

The aim of this study based on theoretical analysis to find out the optimum bed thickness (OBT) of flow-through porous electrode (FTPE) of an electrochemical reactor works under mass transfer regime and for porous bed conductivity

higher than electrolyte ( $k_m \gg k_s$ ) as shown in fig.1.

That is going through reviewing and examining several models accomplished by many authors via experimental data in order to ensure the maximum accuracy and objectivity for such theoretical study.

## 2- MODELS

**2.1. Kreysa [15] in 1978** gave expression for optimum bed depth of packed bed electrode derived from diffusion limiting current density as follows:

$$i_L(x) = aK_m zF \int_x^{L_{op}} [C(x)] dx \quad (1)$$

$$i_L(x) = aK_m zFC(L_{op} - x) \quad (2)$$

For the electrolyte potential  $\phi_s$ , one obtains the expression

$$\phi_s(x) = \int_0^x \frac{i_L(x)}{k_s \varepsilon} dx \quad (3)$$

Substitute eq. 2 into eq. 3 and integrate with boundary condition  $\phi_s(0) = 0$  one obtains

$$\phi_s(x) = \frac{aK_m zFC}{k_s \varepsilon} (L_{op}x - \frac{x^2}{2}) \quad (4)$$

An electrode should be considered as an optimum in the sense explained above if at each point of it  $\geq 99\%$  of limiting current density are realized. Then for packed bed electrode the condition

$$\phi_s(L_{op}) = \eta_{B-F} - \eta_{0.99} \quad (5)$$

Substitute for spherical particles  $a = \frac{6(1-\varepsilon)}{d_p}$  into

eq.4 and rearranging to  $L_{op}$  gives the expression:

$$L_{op} = \left[ \frac{\varepsilon k_s d_p (\eta_{B-F} - \eta_{0.99})}{3(1-\varepsilon)K_m zFC} \right]^{0.5} \quad (6)$$

Where  $L_{op}$ : the optimum bed depth for which limiting current conditions prevail.

$\eta_{0.99}$ : the overvoltage holding the condition when  $i(\eta_{0.99}) = 0.99i_L$

$\eta_{B-F}$ : potential difference between solution potential at the electrode boundary plane nearest the counter electrode and feeder metal potential relative to the equilibrium potential of the electrode reaction.

**2.2 Doherty et al. [2]** showed similar expression as above (eq. 3.39) for penetration depth,  $p$  of the limiting current density for metal deposition (assuming that the electrode is fully conducting) is given by:

$$p = \sqrt{\frac{2\varepsilon k_s \Delta \eta}{aK_m zFC_o}} \quad (7)$$

Where  $\Delta \eta$  is the range of overpotential where the metal deposition proceeds under limiting current conditions.

**2.3 Kreysa et al. (1993)** in more recent study than (1978) showed the optimum bed depth,  $L_{op}$  is given by the following expression:

$$L_{op} = \left( \frac{2k_s \Delta \eta}{a i_L} \right)^{0.5} \quad (8)$$

**2.4 Masliy and Poddubny** (1997) presented the optimum bed thickness in studied the effect of solid and liquid phase conductivity on the effective electrode layer operating under limiting diffusion current.

$$L_d = \sqrt{\frac{2k_s \Delta \eta}{azFK_m C_0}} \quad (9)$$

The four models given above are all the same if some rearrangements are made, except a little difference in eq. 8 where the void fraction is not taken into account. Furthermore, these models based on electrode conductivity much higher than electrolyte ( $k_m \gg k_s$ ).

**2.5 Newman et al.** (1975, 1984 and 1986) introduced the penetration depth,  $p$  as a function of velocity, specific area, and mass transfer coefficient;

$$p = \frac{u}{aK_m} \quad (10)$$

**2.6 Masliy et al.** (1997 & 2007) understood the effectively operating thickness  $L_{eff}$  of porous electrode as a part of its total thickness,  $L$  proportional to the integral mean value of the ratio of local current of the target reaction  $i(x)$ , to its limiting diffusion value  $i_L(x)$ .

$$L_{eff} = \int_0^L \frac{i(x)}{i_L(x)} dx \quad (11)$$

**2.7 Nava et al.** (2008) in a more recent study concerned about determination of the effective thickness of porous electrode in a flow-through porous electrode shows the usefulness type of analysis to estimate the optimum bed thickness from potential distribution which allows efficient recovery of metals by avoiding hydrogen evolution.

$$\phi_s(x) - \phi_s(x=0) = -\frac{zFuC(x=0)}{\nu k_s} [\nu x + \exp^{-\nu x} - 1] \quad (12)$$

Where

$$\nu = \frac{K_m a(1-\varepsilon)}{u} \quad (13)$$

The effective bed thickness obtained can be achieved by plotting the potential distribution (eq. 12) vs. electrode thickness  $L$  before hydrogen evolution starts.

Since the main goal of this study is to find out a mathematical model to represent more suitably

the optimum bed thickness for a FTPE, there are several parameters affecting the optimum bed thickness can be observed from above models. These parameters are 1) electrolyte flow rate; 2) mass transfer coefficient or limiting current density; 3) electrolyte concentration; 4) electrolyte conductivity (and electrode in case ( $k_s = k_m$ )); 5) specific surface area or particle size diameter; 6) electrode void fraction; 7) temperature; and 8) overpotential.

### 3- RESULTS AND DISCUSSION

All the results in this paper represented by several figures have been made as a result of calculations are carried out with aid of experimental data available in order to achieve reasonable and accurate results as possible to examine the models. More information and calculation procedure can be found in Sadeq et al (2009). The discussion takes two prospective sides. The first one discusses the effect of each parameter on the OBT and the second one discusses the efficiency of each model.

#### 3.1 The effect of parameters on the OBT

##### 3.1.1 Electrolyte Flow Rate & Mass Transfer Coefficient

Electrolyte flow rate shows a significant effect on the optimum bed thickness through the considered models and results. In spite of the fact that this parameter is not included in some models (1 – 4; i.e. 2.1 – 2.4 and so on), but its presence strongly affects the results represented by mass transfer coefficient. In addition to the importance of flow rate for such study on optimum bed thickness; many studies take it into account as a main parameter in the analysis which enhances its importance. Figs. (2 and 3) represent the effect of this parameter for many different studies [Bennion & Newman; 1972, Doherty et al.; 1996, El-Deab et al.; 1999, Gaunand et al.; 1977, Lanza & Bertazzoli; 2000] with large range of velocities (0.01 – 7.3 cm/s) based on models (2.1, 2.2, and 2.7). These figs. show that as the flow rate of electrolyte increases the optimum bed thickness decreases. This is evident by the fact that the mass transfer coefficient is greatly affected by flow rate.

Actually, not only the electrolyte flow rate has an effect on the mass transfer coefficient. The mass transfer coefficient is affected by many factors rather than flow rate like diffusivity, temperature, and physical properties of electrolyte,

and that is supported by Wilson and Geankoplis (1966) expressions. Since each reference considered here has its own specific operating conditions, temperature, and the same physical properties, the flow rate of electrolyte shows up as the dominant among these factors.

Also, at low flow rates ( $u \ll 1.0 \text{ cm.s}^{-1}$ ), a new emergence of controlling factor appears, which facilitates the penetration of the process (or maximize the optimum bed thickness) into the porous electrode. This factor is most likely to be the abrupt decrease in the electroactive component concentration over the electrode depth as shown in figs. 3 and 4, and the corresponding increase in the polarizability of the electrode as concluded by Masliy & Poddubny (1997).

Figs. 2 and 3 show in general that increasing flow rate reduces optimum bed thickness, but it is also emphasizing in some way that every single case could be a special one for mass transfer prediction. This can be seen from the style of each curve in the figures of each reference and explains why that is different. The benefits of such study are beyond the scope of broad range of data to make it possible to examine, analyze and study the phenomenon of these factors and parameters.

Briefly, according to models (1 – 4) as the electrolyte flow rates increase the mass transfer coefficient and increase in the limiting current density and consequently decrease the optimum bed thickness. While model 5 by Newman et al. (1975, 1984 and 1986) indicates the opposite to the previous four models, which will be discussed in another section of this paper.

### 3.1.2 Electrolyte Concentration (Reactant)

The effect of concentration on optimum bed thickness can be seen by fig. 4 at various temperatures. The figure shows how the optimum bed thickness decreases as the electrolyte concentration increases at certain temperature and flow rate. This is also true for other temperatures, but further increase in temperature in fig. 4 refers to its effect on optimum bed thickness, not on concentration. Najim's et al. (2006); shows that the temperature has no effect on the concentration, but it affects the physical properties of any solution as well as the electrolyte conductivity in this case.

As shown in fig. 4, the concentration has an observed effect on optimum bed thickness. This effect is calculated from the increasing in limiting

current plateau as electrolyte concentration increases. This is shown by the following equation:

$$i_L = zFK_m C_o \quad (14)$$

The increase in limiting current is due to increase in concentration leads to the observed decrease in optimum bed thickness, Doherty et al (1996).

### 3.1.3 Electrolyte Conductivity & Temperature

Fig. 5 shows the effect of electrolyte conductivity on optimum bed thickness based on Kreysa and Jüttner's data and model. While fig. 6 shows the effect of electrolyte conductivity on optimum bed thickness at various temperatures and concentrations based on Najim's et al (2006) data and Kreysa's (1978) model. These figures show the increase of the optimum bed thickness with increases in electrolyte conductivity. It is also clear that there are some factors which have an effect on the electrolyte conductivity. The figures show that increasing in concentration and temperature leads to increase in the solution conductivity. The reason is beyond the optimum bed thickness as increasing in electrolyte conductivity come from the fact that increasing in electrolyte conductivity means decreasing in electrolyte resistivity, which leads to a decrease in ohmic potential drop in solution, and that decrease leads to increases in electrode polarization which positively is reflected on optimum bed thickness.

It is important to say here that temperature has a considerable effect on electrolyte conductivity which is greater than that of concentration. These effects are shown in figs. 5 and 6. The increase in temperature has been by one magnitude if the concentration doubled, while it is twice if the temperature has increased to 30% of its initial value, this behavior is due to the increase of the solubility of the ions in the electrolyte and its kinetic energy when increasing the temperature. However, all these results are directed up to the evidence that increasing in electrolyte conductivity leads to increasing in optimum bed thickness, and this is also true for temperature which enhances the situation of models (1 – 4).

### 3.1.4 Specific surface Area & Void fraction

Fig. 7 shows the effect of the specific surface area on the optimum bed thickness. The data used in this plotting based on Nava's data and model. The results show that the increase in specific surface area of the porous electrode leads to decreases in the optimum bed thickness according to Nava's

results and model which are considered as a support for what is concluded by models (1 – 4). A little increase in the optimum bed thickness at the right side end of fig. 7 for  $a = 193 \text{ cm}^{-1}$  have been seen. This has happened because of the increasing in void fraction (see the referred reference) which will be seen in fig. 7. This is also true at various flow rates, where fig. 7 shows the effect of specific surface area at more than one condition.

The reason behind that decrease in optimum bed thickness with increases in specific surface area belongs to the fact that porous electrode provides a large space (interfacial area) for the electrochemical reaction, and that enables to take a small volume. Therefore, any additional increase in this part leads to decrease in the optimum bed thickness. This also have been proved by several studies; where, for, e.g., Coeuret et al. (1976 & 1977) found out that the increase in size of particle (for the packing of spherical particles) leads to increase in bed effectiveness which consequently means decrease in the interfacial area.

Since the new types of packing (i.e. RVC, fiber, etc.) make possible to control simultaneously void fraction and specific surface area. Fig. 8 shows how the optimum bed thickness can be strongly affected at certain conditions if the electrode void fraction is made to change. This figure shows the increase in bed void fraction leads to increase in optimum bed thickness according to [2 and 15].

### 3.1.5 Overpotential Difference

The effect of overpotential on optimum bed thickness has been represented in models (1 to 4). Fig. 9 shows polarization curve for a simple electrochemical reaction displaying region where electrode reaction proceeds under mass transport control. Fig. 9 emphasizes that the effect of the overvoltage determined by the width of the limiting current plateau, or in other word, as the overpotential range increases the effect on optimum bed thickness takes a big effect. This effect is indicated regarding models which refer to the increase in overpotential range leads to increases in optimum bed thickness. From practical point of view, that's true since the increase in voltages which represent the driving force for any electrochemical reaction leads to increase in reaction areas and consequently reflects on the penetration depth of the reaction inside pores or which here called optimum bed thickness.

## 3.2 Models Results

### 3.2.1 Kreysa's (1978) and Doherty's et al. (1996), models (1 & 2).

Kreysa's and Doherty's models can be considered as the most appropriate candidates to represent the optimum bed thickness of a FTPE electrochemical reactor operates under mass transfer control. That's because the most effective parameters are represented in these two models and also the results show the most acceptable and reasonable results than others. In addition, models 1 & 2 show a flexibility to interact with different packing type.

It is also important to mention the disadvantages in these two models and the most important one that is related to the overpotential difference (range)  $\Delta\eta$ . The way that has been suggested to represent this parameter by several studies based on the polarization curve when reaction proceeds under mass transfer region. This method could be associated with some mistakes and most likely with such theoretical study. These mistakes usually occur when it has to select a start and end point of the mass transfer region. It has been found that the average approximate error might

occur for this case between  $\mp (50 - 100) \text{ mV}$  in a

worst probability based upon experience, but this range of error can cause a noticeable change in optimum bed thickness appreciable to 6 – 13 % for  $\Delta\eta$  equal to 400 mV and that percent is a candidate to increase as the overpotential range decreases (Sadeq et al. 2009).

The results of these two models (i.e., 1 & 2) are completely matched because they are already matched as mentioned before. The results of these models over the considered experimental data that have been used in the study show a good agreement for all data at high flow rates, while for low flow rates, the results are overestimate for Kreysa (1978) and short bed length (2 cm) for Najim et al (2006). That's probably because the limiting current plateau is so low due to the very low reactant concentration in Kreysa's data which makes the optimum bed thickness represented in these models high even up to or over its actual length. This especially occurs at low flow rates; while the results in short bed length (2 cm) of Najim et al. which overestimating the optimum bed thickness and also the actual bed length probably because of the low specific surface area and flow rates, but even that, the optimum bed thickness



has been found experimentally by Najim et al. between 2 and 3 cm, which are shown up in Sadeq et al. (2009).

The most unfavorable situation occurs for the profile  $\eta(x)$  and  $C(x)$  with the opposite character of behavior, that is, the minimum solution concentration corresponds to the most loaded point of the porous electrode and vice versa (Masliy et al 2007). This makes the attainment of the limiting diffusion current over the entire porous electrode surface difficult, but in this case the reason is the depletion of the solution in the depth of the porous electrode also causes an increase in the polarization resistance at these points and current redistribution towards the less loaded layers. Eventually, this leads to the efficient function of the entire porous electrode (maximum optimum bed achieved) and that which appears in [Newman and Matloz (1986), Kreysa (1978), and Najim et al. (2006)] at so low flow rates, but it is more costly because of the lower flow rate, high current overload and decrease in the current efficiency (Masliy et al. 2007). However, the average optimum bed thickness over the total results at six different flow rates of Kreysa (1978) about 2.37 cm, which is approximately the actual bed length (2.3 cm) for that case. In addition, a comparison of specific surface area  $a = 5.66 \text{ cm}^{-1}$  of Najim et al. (2006) within that used for example by Kreysa (1978)  $a = 36 \text{ cm}^{-1}$  or Newman (1986)  $a = 66 \text{ cm}^{-1}$ , shows how it is small for such application to be justified by high interfacial area. From practical point of view and according to reasons mentioned above, it can be concluded that results reflect the whole bed are considered as an optimum more than its value.

## 2-Kreysa and Jüttner's (1993) & Masliy and Poddubny's (1997), Models (3 & 4)

These two models are so close to that predicted by Kreysa (1978) and Doherty et al. (1996), the differences only by ignoring the void fraction  $\varepsilon$  as mentioned before. But this neglected parameter causes a dramatic change in the results compared with the previous models (1 & 2). These changes or effects of this parameter can be seen through figs. (10 – 13). Figs. (10 – 13) show the variation or difference between models 1 and 2, and models 3 and 4 are proportional to or justified by  $(1 - \varepsilon)^{0.5}$ . As the void fraction decreases the differences between the models curves increase and that would vindicate the variation of the shifting ratio among the referred figures.

Furthermore, these figs. emphasize the importance of that parameter and its effect on the optimum bed thickness. Fig. 13 shows how much close could be between models 1 and 2, and 3 and 4 if the void fraction is high, which reflects perhaps the reason beyond the neglecting of this parameter especially before the most recent studies concentrated to use new types of packing that provides simultaneously high specific surface area and void fraction.

One more thing, in spite of these two models sometimes overestimate the optimum bed thickness when the void fraction is small and even overestimate the actual bed length.

The surprising thing about these models is even that overestimating results, but it never overtakes the rules of model 7 (i.e. exceeding the side reaction value or hydrogen evolution start) that predicted by Nava et al. (2008), as shown in figs. 15 and 16. Everything else mentioned about these models is all that is mentioned in discussion about models 1 and 2.

## 3.2.3 Newman's et al. (1975, 1984 and 1986), Model 5.

The behavior of this model shows variant behavior compared to other models that have been accomplished by [Doherty et al. 1996, Kreysa 1978, Masliy et al. 1997 and Nava et al. 2008] rather than un-reasonable results in many parts. Even that, this variant does not represent the evident scientific mechanisms. But from another point of view, one can notice that the results obtained from the same data source of (Newman and Matloz 1986) or from data have the same conditions is quite reasonable values and that obviously seen in fig. 14 and that's most likely for low velocities and high specific surface area. However, fig. 14 also shows variant behavior in model 5 to that shown in model 7 and the other four models (i.e. the optimum bed thickness increases as the velocity). That could happen at typical conditions of so low flow rates. The poor representation of the parameters and the variant behavior does not give the possibility for considering this model to express the optimum bed thickness of a FTPE under wide range of conditions. However, from other point of view, the reason which makes Newman [6, 19, and 20] to consider that represent the penetration depth at first, perhaps because it is a simple model that might give a quick estimation with percent of error for a certain situation, and that's most likely with high specific surface areas

and low flow velocities [6, 20] as mentioned before.

### 3.2.4 Masliy's et al. (1997, 2007), Model 6

Unfortunately, there are no experimental data to meet this theoretical model which requires to be executed as a fair action in the present study, in order to make sure to show the method of solution and to cover all the models. A test of this model has been made from a theoretical data based on a simulation study in Sadeq et al. (2009).

### 5.2.5 Nava's et al. [26], Model 7

The result of this model which is completely graphical shows a good way to estimate the optimum bed thickness through the entire results. The behavior indicated in this model agreed with that of models 1–4 which are supported by figs. 4.5 and 4.9. The major idea of this model based on Coulombic efficiency calculations. As the Coulombic efficiency of the reaction is 100%, the bed is considered optimum at that efficiency. The Coulombic efficiency  $\psi$  can be defined as the percentage of the measured current supported by the main deposition reaction [17], i.e.

$$\psi = \frac{i_{main}}{i_{main} + i_{side}} \times 100\% \quad (15)$$

Since model 7 is already adopted, then all the optimum bed thickness obtained from this model operates with 100% Coulombic efficiency according to eq. 15. One more thing, the results of optimum bed thickness obtained from model 7 is always greater than that for models 1–4, that are evident between figs. 15 and 16. This reflects two facts, the first is that model 7 represents a range wider than mass transfer region, and the second is the validity of models 1–4 to represent the optimum bed thickness in the mass transfer region (especially model 1 and 2), and avoiding the side reaction.

## 4- CONCLUSIONS

The increase in electrolyte flow rate, mass transfer coefficient, concentration, limiting current density, and specific surface area reduces the optimum bed thickness. The increase in electrolyte conductivity, porosity, and overpotential range increases optimum bed thickness. The first four models (1–4) can be used with relatively high flow rates and specific surface area ( $u \geq 0.1$  cm/s,  $a \geq 12$  cm<sup>-1</sup>). The best models among the first four that have been tested are models 1 and 2

predicted by Kreysa (1978) and Doherty et al. (1996) to represent the optimum bed thickness for reactor operating under mass transfer control. Models 3 and 4 predicted by Kreysa and Jüttner (1993) and Masliy and Poddubny (1997) are used to estimate the optimum bed thickness when bed porosity is high ( $\varepsilon \geq 0.9$ ). Model 5 predicted by Newman et al. (1975, 1984 and 1986), can be used for low flow rates and high specific surface area ( $u < 0.09$  cm/s,  $a \geq 25$  cm<sup>-1</sup>). The graphical model presented by Nava et al. (2008) can be a useful way to use in processes when high degrees of conversion are required per pass. The exact value of the optimum bed thickness cannot be deduced analytically, but model 1 gives a first approximation value which can be useful for a rough engineering design. The bed of a FTPE can be whatever size in diameter, but the thickness of the reactor is very important to take into account for this configuration.

## NOMECULATURE

$a$	Specific surface area of electrode; (cm <sup>-1</sup> )
$C$	Electrolyte concentration; (mol/cm <sup>3</sup> )
$C_o$	Inlet electrolyte concentration; (mol/cm <sup>3</sup> )
$d_p$	Size diameter of spherical particle; (cm)
$F$	Faraday's constant (96,487); (C/g.equ.)
$i_o$	Exchange current density; (A/cm <sup>2</sup> )
$i$	Current density; (A/cm <sup>2</sup> )
$i_L$	Limiting current density; (A/cm <sup>2</sup> )
$K_m$	Mass transfer coefficient; (cm/s).
$k_m$	Solid phase conductivity; ( $\Omega$ cm) <sup>-1</sup>
$k_s$	Effective electrolyte conductivity; ( $\Omega$ . cm) <sup>-1</sup>
$L$	Electrode length; (cm)
$L_d$	Thickness of porous electrode layer operating at the limiting diffusion current as in eq. 9; (cm).
$L_{eff}$	Effective operating thickness as in eq. 11; (cm).
$L_{op}$	Optimum bed length (cm).
$P$	Penetration depth as in eq. 10; (cm)
$p$	Penetration depth as in eq. 7; (cm)
$R$	Gas constant = 8.314 (J/mol. K)
$T$	Temperature (K)
$u$	Electrolyte flow rate (cm/s)
$V_c$	Applied potential at the cathode current feeder (or collector); (Volt)
$z$	Number of electrons involved in reaction

## GREEK LETTERS

$\varepsilon$	Void fraction
$\eta$	Overpotential
$v$	Group parameter defined in eq. 3.19
$\phi_m$	Electrode potential
$\phi_s$	Electrolyte potential
$\psi$	Coulombic efficiency defined in eq. 15





## REFERENCES

- Bennion, D. N., Newman, J., "Electrochemical removal of copper ions from very dilute solutions" *J. Appl. Electrochem.* **2**, 133, (1972).
- Coeuret, F., Hutin, D., Gaunand, A., "Study of the effectiveness of fixed flow-through electrodes" *J. Appl. Electrochem.* **6**, 417 (1976).
- Doherty, T., Sunderland, J.G., Roberts, E.P.L., Pickett, D.J., "An improved model of potential and current distribution within a flow-through porous electrode" *Electrochim. Acta.* **41** (4), 519 (1996).
- El-Deab, M. S., Saleh, M. M., El-Anadoul, B., E., Ateya, B. G., "Electrochemical removal of lead ions from flowing electrolytes using packed bed electrodes" *J. Electrochem. Soc.* **146** (1), 208 (1999).
- Gaunand, A. Hutin, D. and Coeuret, F., "Potential distribution in flow-through porous electrodes under limiting current" *Electrochim. Acta.* **22**, 93 (1977).
- Kreysa, G., "Kinetic behavior of packed bed and fluidized bed electrodes" *Electrochim. Acta.* **23**, 1351 (1978).
- Kreysa, G., Reynvaan, C., "Optimal design of packed bed cells for high conversion" *J. Appl. Electrochem.* **12**, 241 (1982).
- Kreysa, G., Jüttner, K., "Cylindrical three-dimensional electrodes under limiting current conditions" *J. Appl. Electrochem.* **23**, 707 (1993).
- Lanza, M.R.V., Bertazzoli, R., "Removal of Zn(II) from chloride medium using a porous electrode: current penetration within the cathode" *J. Appl. Electrochem.* **30**, 61 (2000).
- Masliy, A.I., Poddubny, N.P., "influence of solid phase conductivity on spatial localization of electrochemical processes in flow-through porous electrodes" *J. Appl. Electrochem.* **27** (9) 1036 (1997).
- Masliy, A. I., Poddubny, N. P., Medvedev, A. Zh., Zherebilov, A. F., "Modeling of the dynamics of metal deposition inside a flow-through porous electrode with low initial conductivity" *J. Electroanalytical Chemistry.*
- Matloz, M.J., Newman, J., "Experimental investigation of a porous carbon electrode for the removal of mercury from contaminated brine" *J. Electrochem. Soc.* **133** (9), 1850 (1986).
- Najim, S. T., Kashmoula, T. B., Slaiman, Q. J. "Laboratory scale production of *p*-aminophenol using electrochemical reactor" Ph.D. thesis, *Nahrain University* (2006).
- Nava, J.L., Oropeza, M.T., Ponce de León, C., González-García, J., Frías-Ferrer, A. J., "Determination of the effective thickness of a porous electrode in a flow-through reactor; effect of the specific surface area of stainless steel fibres, used as a porous cathode, during the deposition of Ag(I) ions" *Hydrometallurgy.* **91**, 98 (2008).
- Newman, J., Tiedemann, W., "Porous-electrode theory with battery applications" *AIChE Journal.* **21** (1), 25 (1975).
- Newman, J., Risch, T., "A theoretical comparison of flow-through and flow-by porous electrode at the limiting current" *J. Electrochem. Soc.* **131** (11), 2551 (1984).
- Paulin, M., Hutin, D., Coeuret, F., "Theoretical and experimental study of flow-through porous electrodes" *J. Electrochem. Soc.* **124** (2), 180 (1977).
- Podlaha, E.J., Fenton, J.M., "Characterization of a flow-by RVC electrode reactor for the removal of heavy metals from dilute solutions". *J. Appl. Electrochem.* **25**, 299 (1995).
- Ponce de León, C., Pletcher, D., "The removal of Pb(II) from aqueous solutions using a reticulated vitreous carbon cathode cell—the influence of the electrolyte medium". *Electrochim. Acta* **41** (4), 533 (1996).
- Sabacky, B.J., Evans, J.W., "Electrodeposition of metals in fluidized bed electrodes Part I. Mathematical model". *J. Electrochem. Soc.* **126**, 1176 (1979).
- Sadeq A. A., Najim, S. T., Slaiman, Q. J. "Theoretical analysis of the optimum bed thickness of an electrochemical reactor" M.Sc. thesis, *Nahrain University* (2009).

Saleh, M.M., "On the effectiveness factor of flow-through porous electrodes" *J. Phys. Chem.*, **B 108**, 13419 (2004).

Soltan, E.A., Nosier, S.A., Salem, A.Y., Mansour, I.A.S., Sedahmed, G.H., "Mass transfer behaviour of a flow-by fixed bed electrochemical reactor under different hydrodynamic conditions". *Chem. Eng. J.* **91**, 33 (2003).

Sioda R. E., "Distribution of potential in a pore electrode under conditions of flow electrolysis" *Electrochim. Acta.* **16**, 1569 (1971).

Trainham, J. A. and Newman, J., "A flow-through porous electrode model: Application to metal-ion removal from dilute streams" *J. Electrochem. Soc.* **124** (10), 1528 (1977).

Wilson, E. J., Geankoplis, C. J., *Ind. Eng. Chem. Fund.* **5**, (1966).

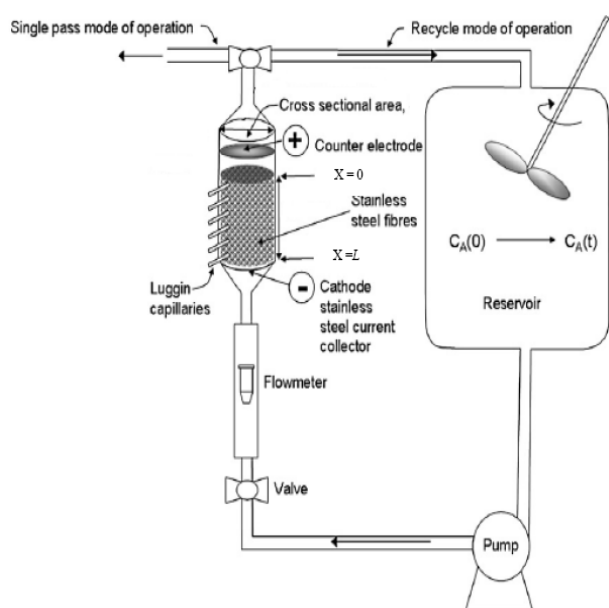


**Fig. 1** Experimental flow circuit and flow-through packed bed electrochemical reactor; Nava (2008).

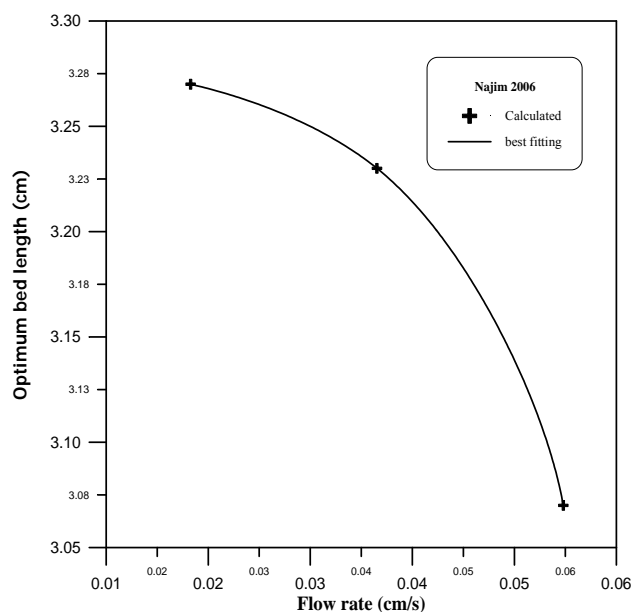


**Fig. 2** Effect of flow rate on OBT, Najim et al. (2006) data based on models (1&2).

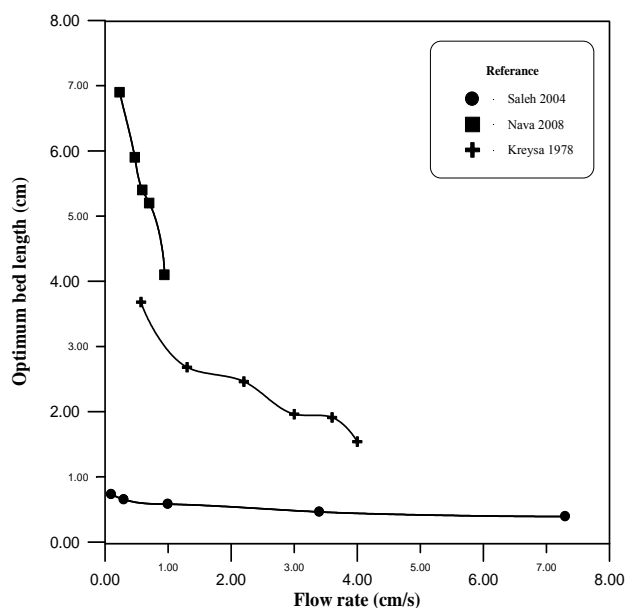


**Fig. 3** Effect of flow rate on OBT based on models (1, 2, and 7).

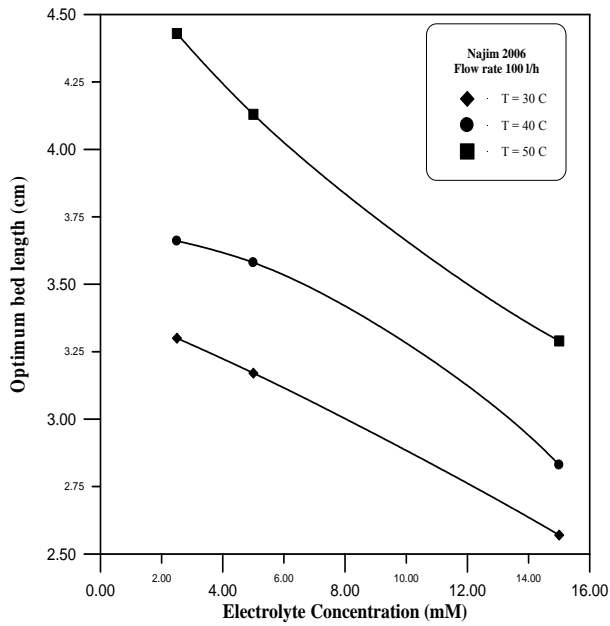


**Fig. 4** Effect of electrolyte concentration on OBT at various temperatures [Najim et al. (2006) data].

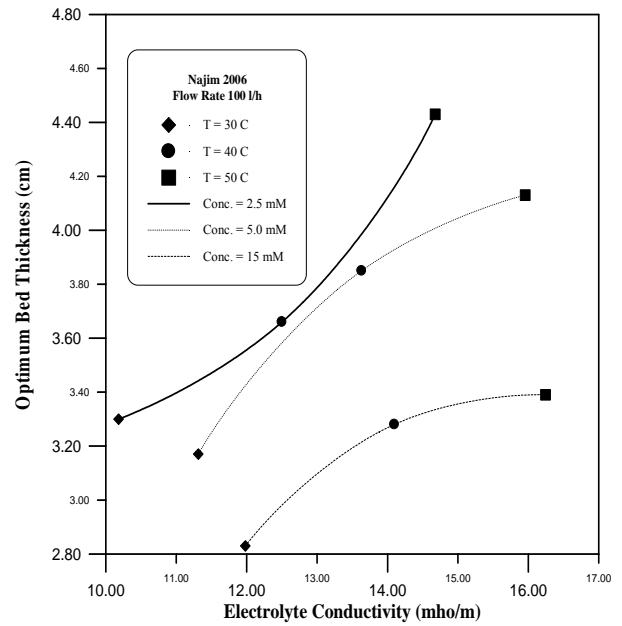


**Fig. 6** Effect of electrolyte conductivity on OBT from Najim (2006) data.

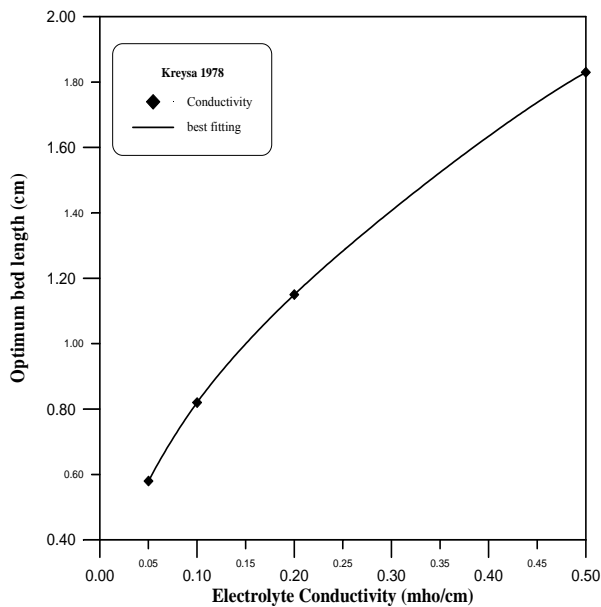


**Fig. 5** Effect of electrolyte conductivity on OBT [Kreysa and Jüttner].

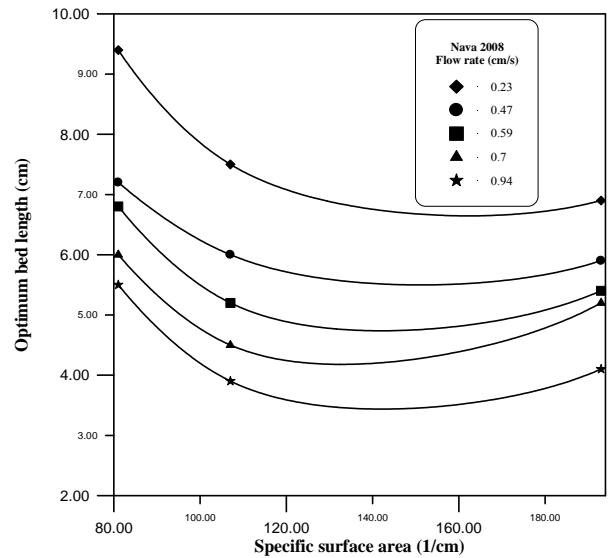


**Fig. 7** Effect of specific surface area on OBT at various flow rates from Nava's (2008) data.

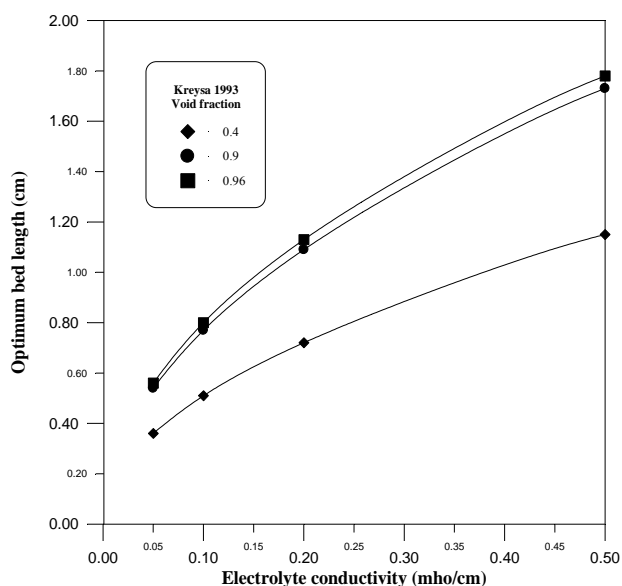


**Fig. 8** Effect of void fraction on OBT at various conductivities from Najim's (2006) data.

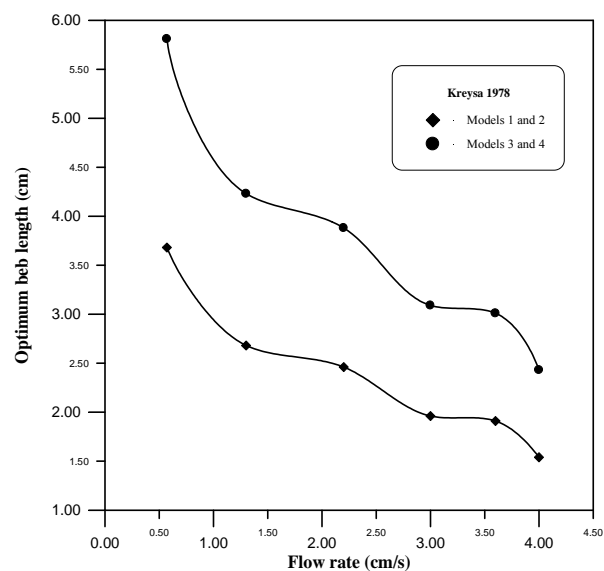
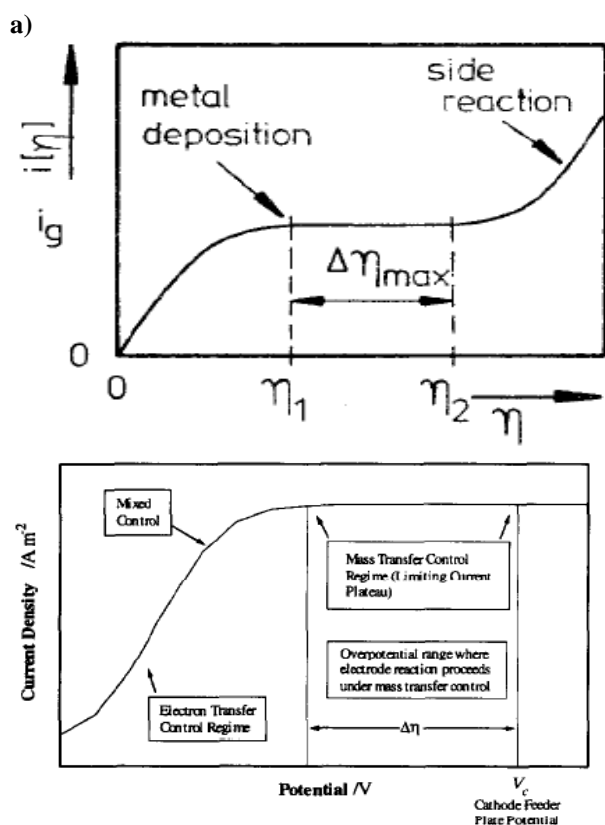


**Fig. 10** Models comparison based on Kreysa's (1978) data.



**b)**

**Fig. 9** Polarization curve for a simple electrochemical reaction **a)** Kreysa and Reynvaan (1982), **b)** Doherty et al. (1996).

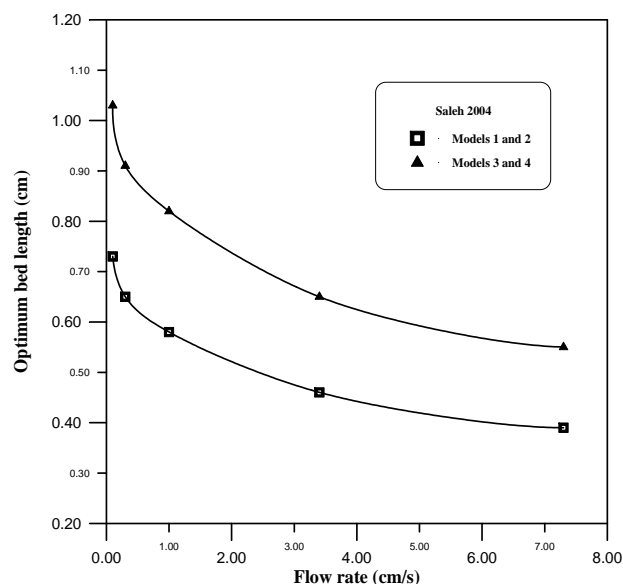


**Fig. 11** Models comparison based on Saleh's (2004) data.

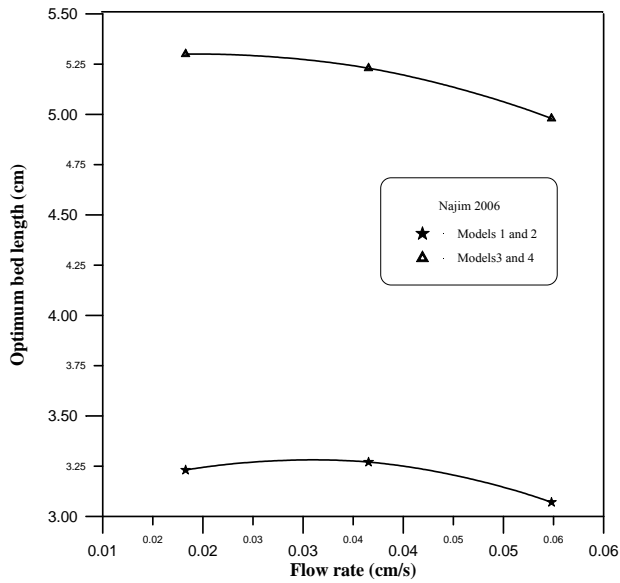


**Fig. 12** Models comparison based on Najim's et al. (2006) data.

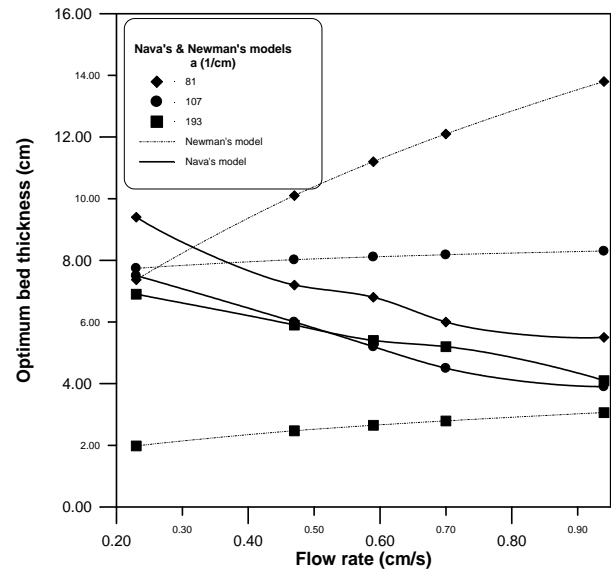


**Fig. 14** Comparison between Newman's (1986) and Nava's (2008) models

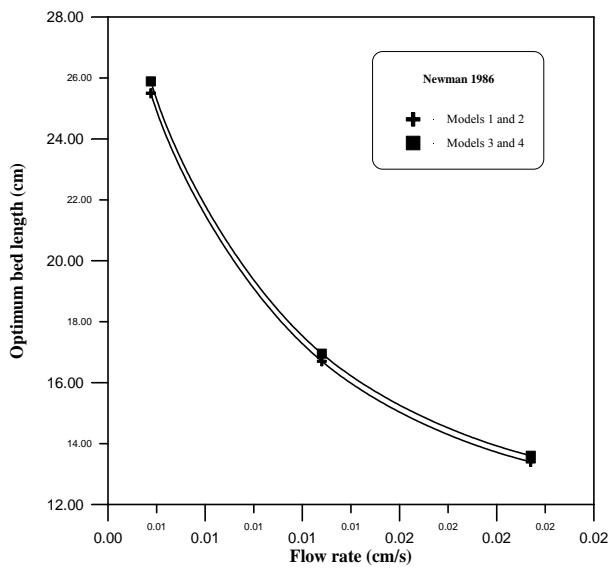


**Fig. 13** Models comparison based on Newman's (1986) data.

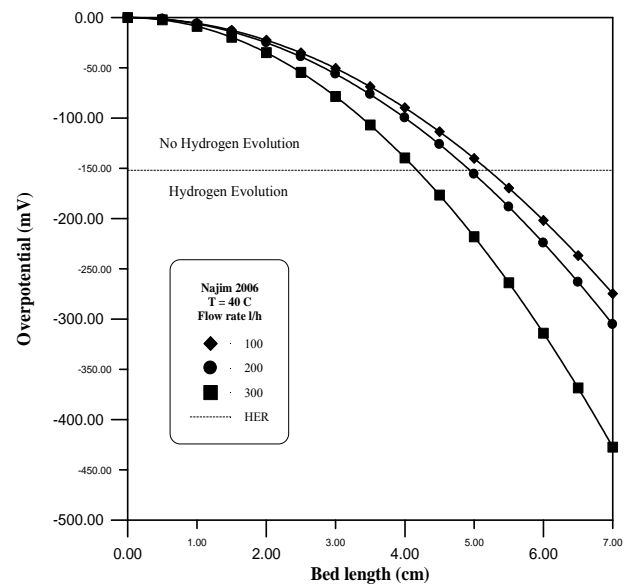


**Fig. 15** Potential distribution for bed length  $L = 7$  cm,  $[\text{Fe}^{3+}] = 15\text{mM}$  based on model 7; eq. 12.

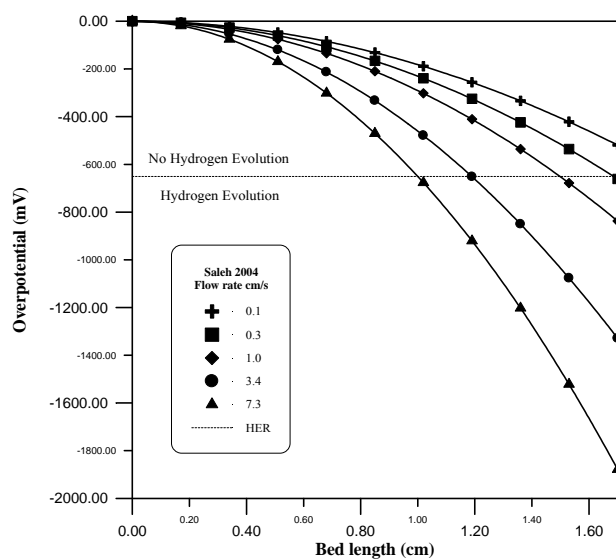


**Fig. 16** Potential distribution for bed length  
 $L=1.7$ cm based on model (7) eq. 12.